Hindawi
Wireless Communications and Mobile Computing
Volume 2019, Article ID 7985414, 7 pages
https://doi.org/10.1155/2019/7985414

Research Article

Sum Rate of Multiuser Large-Scale MIMO in the Presence of Antenna Correlation and Mutual Coupling

Yusheng Li,[1] Kang An,[1] Tao Liang,[1] and Weixin Lu[2]

[1]*National University of Defense Technology, China*
[2]*College of Communications Engineering, Army Engineering University, Nanjing, China*

Correspondence should be addressed to Kang An; ankang@nuaa.edu.cn

Received 21 January 2019; Revised 5 May 2019; Accepted 28 May 2019; Published 13 June 2019

Academic Editor: Jun Cai

A multiuser large-scale MIMO system with antenna correlation and mutual coupling is investigated in this paper. Based on the maximum signal-to-interference-plus-noise ratio (SINR) criteria, the optimal beamforming (BF) vector at the base station (BS) for each user is first obtained using statistical channel state information (CSI). Then, a closed-form expression for the achievable sum rate is derived in terms of a finite number of generalized Meijer-G functions, which is applicable to an arbitrary number of array elements and/or users, and provides an efficient means of evaluating the system performance. Finally, numerical results are provided to confirm the validity of the theoretical analysis and show the impact of various channel parameters on the system performance.

1. Introduction

The pursuit of higher throughput and reliability has established multiple-input multiple-output (MIMO) technology an integral part of many advanced wireless communication systems. The application of MIMO in cellular architectures, including techniques such as multiuser MIMO (MU-MIMO), has gained significant research interest since it can offer spatial multiplexing gain even if each user only has a single antenna [1]. In such systems, a base station (BS) employed with multiple antennas simultaneously serves a number of cochannel users. In order to address the need for even greater capacity in future wireless networks, large-scale MIMO (LS-MIMO) or massive MIMO has been considered as a promising candidate to substantially improve spectral efficiency for next generation wireless systems. Unlike conventional small-scale MIMO systems (e.g., the LTE standard allows for only up to 8 antennas), massive MIMO suggests the use of hundreds of antennas at the BS, serving dozens of users at the same time [2–5].

In practical large-scale MIMO systems, however, a limited array aperture coupled with a large number of antennas may result in two major concerns: antenna correlation and mutual coupling (MC) effects. It is well-known that antenna correlation often exists in many practical environments due to insufficient antenna spacing and/or lack of scattering [6]. In addition, limited spacing between antenna elements in an array is also responsible for the mutual coupling, which can degrade signal transmission and reception due to antenna impedance mismatch [7]. The effects of antenna correlation and mutual coupling on traditional MIMO systems have been well-studied in [8–14], where the antenna arrays are commonly restrained less than 8×8 elements. Specifically, the authors in [8] applied random matrix theory to obtain analytical characterizations of the capacity of correlated multiantenna channels. In [9], the effects of fading correlations on MIMO systems were investigated by introducing the concept of sample-mean outage and information theoretic measures. The work in [10] analyzed the achievable rate of MIMO systems in the presence of mutual coupling and spatial correlation, which consisted of dipole antennas placed side-by-side in a linear pattern and in a very limited physical space. In [11], the impact of mutual coupling induced by two closely spaced minimum scattering antennas at the subscriber unit on 2 × 2 MIMO systems was investigated, where both (de)correlation effects and variations of antenna gain resulting from coupling mechanisms were considered. The authors in [12] addressed the question of how coupling impacts

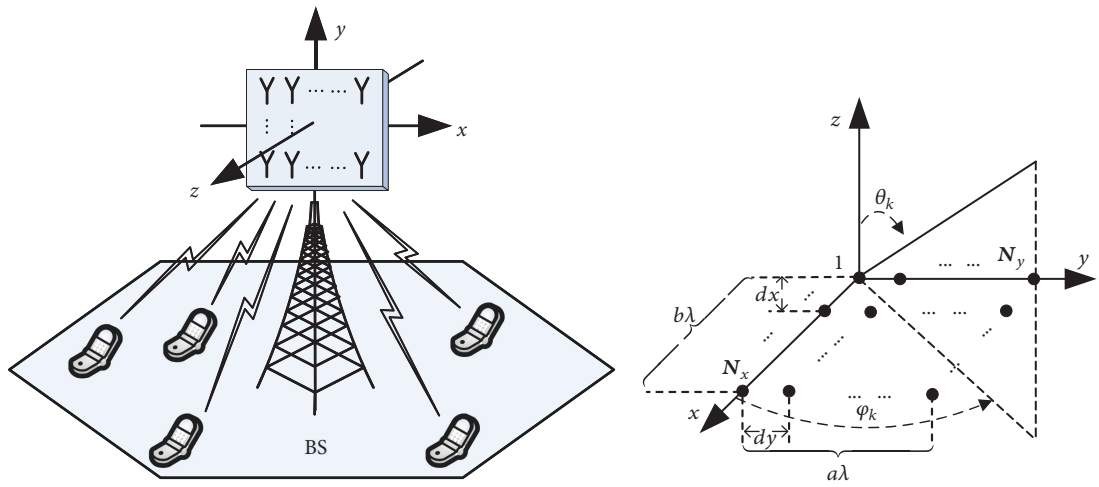

(a) Uplink multiuser large-scale MIMO system

(b) Diagram of $N_x \times N_y$ URA

Figure 1: System model.

bandwidth in the context of circular arrays. Moreover, the impact of mutual coupling on LTE-R MIMO capacity for antenna array configurations in high speed railway scenario was investigated in [13]. The authors in [14] provided a systematic review of the mutual coupling in MIMO systems, including the effects on performances of MIMO systems and various decoupling techniques.

By invoking a large number of antenna elements, massive MIMO or large-scale array has been viewed as a critical technique to overcome the combined effect of the mobile data traffic soaring trend and the favorable radio spectrum scarcity for the forthcoming communication systems which brings significant advantages including higher spectral efficiency, reduced radiated power consumption, and greater simplicity in signal processing. Considering both the antenna correlation and mutual coupling, the authors in [15] have investigated the performance of multiuser massive MIMO systems with uniform linear arrays (ULAs). The authors in [16] analyzed the performance of multiuser massive ULA MIMO Systems with mutual coupling calibration. Besides, the effect of mutual coupling in ULA large-scale antenna array with frugal calibration was studied in [17]. Compared with ULAs, uniform rectangular arrays (URAs) or uniform circular arrays (UCAs) are more space-efficient and offer numerous advantages [18]. Therefore, [19] has explored the impact of mutual coupling on uplink multiuser massive MIMO systems with a URA. Nevertheless, these aforementioned works assume perfect channel state information must be available at the BS, which is too restrictive in practice owing to fast fading, limited training sequences, and the heavy feedback burden.

Motivated by the aforementioned observations, this paper investigates the performance of an uplink multiuser large-scale MIMO system in the presence of both antenna correlation and mutual coupling. Particularly, the contribution of this work can be summarized as follows.

(i) Considering both the antenna correlation and mutual coupling, we establish a general framework of multiuser massive MIMO systems with URA. Compared to the existing works limited to the perfect CSI cases, our work employs statistical CSI to evaluate the system performance more practically.

(ii) Based on the statistical CSI at the BS, we first formulate the maximum signal-to-interference-plus-noise (SINR) based optimization problem and obtain the optimal beamforming vector for each user by using the Rayleigh quotient. Using the generalized Meijer-G functions, a closed-form expression for the achievable sum rate of the large-scale MIMO system is derived.

(iii) Theoretical analysis is confirmed through comparison with simulation results, and the effect of antenna correlation and mutual coupling on the LS-MIMO system is investigated. The findings in this work provide a useful guidance for the system design and performance evaluation of massive MIMO systems with joint antenna correlation and mutual coupling in the presence of imperfect CSI.

The rest of this paper is organized as follows. The system under consideration is described in Section 2. In Section 3, the channel statistical properties used to evaluate its performance are provided. In Section 4, the closed-form expression for the achievable sum rate is derived. Simulation and numerical results are presented in Section 5. Finally, conclusions are drawn in Section 6.

2. System Model

We consider an uplink multiuser large-scale MIMO system as shown in Figure 1, where a BS equipped with an N-element URA receives signals from K single antenna users.

The users are assumed to be randomly located within a single cell according to a uniform distribution, and the size of the URA is assumed to be $a\lambda \times b\lambda$ with λ being wavelength of the transmitted signal, and a and b are the length and width of the URA in wavelengths, respectively. The number of elements in the azimuth and elevation dimensions are N_x and N_y, respectively. Therefore, we have $d_x = a\lambda/(N_x - 1)$ and $d_y = b\lambda/(N_y - 1)$ and $N = N_x N_y$.

2.1. Uplink Multiuser Large-Scale MIMO System. In this paper, we focus on the uplink of multiuser large-scale MIMO systems, where the received signal at the BS can be expressed as

$$\mathbf{y} = \mathbf{H}\mathbf{P}^{1/2}\mathbf{s} + \mathbf{n}, \tag{1}$$

where $\mathbf{H} = [\mathbf{h}_1, \mathbf{h}_2, \ldots, \mathbf{h}_K]$ denotes the channel matrix with $\mathbf{h}_k$ being the channel vector between the k-th user and BS, and $\mathbf{P} = \mathrm{diag}(p_1, p_2, \cdots, p_K)$ with p_k representing the transmit power of the k-th user. The vector $\mathbf{n}$ represents zero mean additive white Gaussian noise (AWGN) satisfying $\mathbf{n} \sim \mathcal{N}_C(\mathbf{0}_N, \mathbf{I}_N)$, and $\mathbf{s} = [s_1, s_2, \cdots, s_K]^T$ is the vector of the individual symbols simultaneously transmitted by the K users.

Throughout this paper, all the wireless channels are assumed to experience cluster-based correlated fading, which is a widely adopted channel model for the outdoor propagation environment [6]. In this model, the channel vector between the k-th user and BS can be written as

$$\mathbf{h}_k = \sum_{l=1}^{L_k} \rho_{k,l} \mathbf{a}_k(\theta_{k,l}, \varphi_{k,l}), \tag{2}$$

where L_k is the total number of multipath signals, and $\rho_{k,l}$ represents the fading coefficient of the l-th path channel. The vector $\mathbf{a}_k(\theta_{k,l}, \varphi_{k,l})$ denotes the 2D array steering vector for a N- element URA, which can be rewritten as

$$\mathbf{a}_k(\theta_{k,l}, \varphi_{k,l}) = \mathbf{a}_{k,N_x}(\theta_{k,l}) \otimes \mathbf{a}_{k,N_y}(\varphi_{k,l}), \tag{3}$$

where the p,q-th $(p = 1, 2, \ldots, N_x)$ $(q = 1, 2, \ldots, N_y)$ element of the $\mathbf{a}_k(\theta_{k,l}, \varphi_{k,l})$ can be expressed as [20]

$$a_k^{(p,q)}(\theta_{k,l}, \varphi_{k,l}) = \exp\left\{ j\kappa \left[d_x(p-1)\sin\theta_{k,l}\cos\varphi_{k,l} + d_y(q-1)\sin\theta_{k,l}\sin\varphi_{k,l} \right] \right\}, \tag{4}$$

where κ is the wave number, $\theta_{k,l} \in [\theta_k - \Delta\theta_k/2, \theta_k + \Delta\theta_k/2]$ and $\varphi_{k,l} \in [\varphi_k - \Delta\varphi_k/2, \varphi_k + \Delta\varphi_k/2]$, respectively, represent the azimuth and elevation angle of arrival of the l-th path signal, with θ_k and ϕ_k indicating the mean of angle-of-arrival (AOA), and $\Delta\theta_k$ and $\Delta\varphi_k$ are the corresponding angular spreads.

2.2. Channel Modeling. With the above array model and assuming mutual coupling, the correlated channel vector of the k-th user can be expressed as [6, 15, 19]

$$\mathbf{h}_k = \mathbf{C}\mathbf{R}_k^{1/2}\widetilde{\mathbf{h}}_k, \tag{5}$$

where

(i) $\mathbf{R}_k$ denotes the channel correlation matrix (CCM) of each link, which is given by

$$\mathbf{R}_k = \sum_{l=1}^{L_k} \mathrm{E}\left[|\rho_{k,l}|^2 \right] \mathbf{a}_k(\theta_{k,l}, \varphi_{k,l}) \mathbf{a}_k^H(\theta_{k,l}, \varphi_{k,l}), \tag{6}$$

with the eigendecomposition of the CCM being given by

$$\mathbf{R}_k = \mathbf{U}_k \mathbf{\Sigma}_k \mathbf{U}_k^H, \tag{7}$$

where $\mathbf{\Sigma}_k = \mathrm{diag}(\lambda_{k,1}, \lambda_{k,2}, \cdots \lambda_{k,N})$ is a diagonal matrix with the eigenvalues $\lambda_{k,n}$ arranged in a non-increasing order, and $\mathbf{U}_k = [\mathbf{u}_{k,1}, \mathbf{u}_{k,2}, \cdots, \mathbf{u}_{k,N}]$ are the corresponding eigenvectors.

(ii) $\widetilde{\mathbf{h}}_k = [\widetilde{h}_{k,1}, \widetilde{h}_{k,2}, \cdots, \widetilde{h}_{k,N}]^T$ has independent identically distributed (i.i.d) entries following $\widetilde{\mathbf{h}}_k \sim \mathcal{N}_C(\mathbf{0}_N, \mathbf{I}_N)$.

The mutual coupling matrix can be calculated by using the following relationship involving the impedance matrix as [15]

$$\mathbf{C} = (Z_A + Z_T)(\mathbf{Z} + Z_T\mathbf{I}_N)^{-1}, \tag{8}$$

where Z_A and Z_T denote the antenna impedance and load impedance, respectively. According to the URA in Figure 1, the mutual impedance matrix $\mathbf{Z}$ can be described by

$$\mathbf{Z} = \begin{bmatrix} Z_A & Z_{21} & \cdots & Z_{1N} \\ Z_{12} & Z_A & \cdots & Z_{2N} \\ \vdots & \vdots & \ddots & \vdots \\ Z_{N1} & Z_{N2} & \cdots & Z_A \end{bmatrix}, \tag{9}$$

Where, for a side-by-side array configuration of wire dipoles, $[\mathbf{Z}]_{m,n}$ can be determined using the classical induced electromotive force (EMF) method in [21].

2.3. Beamforming Scheme with Statistical CSI. The received signals are separated into individual data streams by multiplying with the linear detector $\mathbf{W}$ as

$$\widetilde{\mathbf{y}} = \mathbf{W}^H\mathbf{y}, \tag{10}$$

where $\mathbf{W}$ denotes the $N \times K$ beamforming matrix. For the purpose of our performance analysis, we write the output signal of the k-th user after beamforming as

$$\widetilde{y}_k = \underbrace{\sqrt{p_k}\mathbf{w}_k^H\mathbf{h}_k s_k}_{\text{desired signal}} + \underbrace{\sum_{j=1, j\neq k}^{K} \sqrt{p_j}\mathbf{w}_k^H\mathbf{h}_j s_j}_{\text{co-channel interference}} + \underbrace{\mathbf{w}_k^H\mathbf{n}}_{\text{noise}}, \tag{11}$$

where $\mathbf{w}_k$ and $\mathbf{h}_k$ are the k-th columns of the beamforming matrix $\mathbf{W}$ and channel matrix $\mathbf{H}$, respectively. By considering

both of the channel correlation and mutual coupling effects, the average output SINR can be expressed as

$$\mathrm{E}\left[\gamma_k\right] = \frac{p_k \mathbf{w}_k^H \mathbf{C}\mathbf{R}_k \mathbf{C}^H \mathbf{w}_k}{\mathbf{w}_k^H \mathbf{C}\left[\sum_{j=1,j\neq k}^{K} p_j \mathbf{R}_j\right]\mathbf{C}^H \mathbf{w}_k + \sigma^2 \mathbf{I}_N}, \quad (12)$$

where we have applied the fact that

$$\begin{aligned} \mathbf{R}_k^{H/2} &= \mathbf{R}_k^{1/2}, \\ \mathrm{E}\left[\widetilde{\mathbf{h}}_{\mathrm{k}} \widetilde{\mathbf{h}}_{\mathrm{k}}^{\mathrm{H}}\right] &= \mathbf{I}_{\mathrm{N}}, \end{aligned} \quad (13)$$

and obtain

$$\mathrm{E}\left[\mathbf{h}_k \mathbf{h}_k^H\right] = \mathrm{E}\left[\mathbf{C}\mathbf{R}_k^{1/2} \widetilde{\mathbf{h}}_k \widetilde{\mathbf{h}}_k^H \mathbf{R}_k^{H/2} \mathbf{C}^H\right] = \mathbf{C}\mathbf{R}_k \mathbf{C}^H, \quad (14)$$

$$\begin{aligned} &\mathrm{E}\left[\sum_{j=1,j\neq k}^{K} p_j \mathbf{h}_j \mathbf{h}_j^H\right] \\ &= \mathrm{E}\left[\sum_{j=1,j\neq k}^{K} p_j \mathbf{C}\mathbf{R}_j^{1/2} \widetilde{\mathbf{h}}_j \widetilde{\mathbf{h}}_j^H \mathbf{R}_j^{H/2} \mathbf{C}^H\right] \\ &= \mathbf{C}\left(\sum_{j=1,j\neq k}^{K} p_j \mathbf{R}_j\right)\mathbf{C}^H, \end{aligned} \quad (15)$$

$$\mathrm{E}\left[\mathbf{n}\mathbf{n}^H\right] = \sigma^2 \mathbf{I}_N. \quad (16)$$

Proposition 1. *Suppose* $\mathbf{A}$ *and* $\mathbf{B}$ *are the two* $N \times N$ *sized Hermitian matrices, and* $\mathbf{B}$ *is positive definite; the following inequality holds [22]:*

$$\frac{\mathbf{x}^{\mathrm{H}} \mathbf{A}\mathbf{x}}{\mathbf{x}^{\mathrm{H}} \mathbf{B}\mathbf{x}} \leq \lambda_{max}\left(\mathbf{B}^{-1}\mathbf{A}\right) \quad (17)$$

The inequality is satisfied with equality at the optimum only when

$$\mathbf{x}^{opt} = c\mathbf{u}_{max}\left(\mathbf{B}^{-1}\mathbf{A}\right) \quad (18)$$

where c *can be any nonzero constant. In the above equations,* $\lambda_{max}\left(\mathbf{B}^{-1}\mathbf{A}\right)$ *and* $\mathbf{u}_{max}\left(\mathbf{B}^{-1}\mathbf{A}\right)$ *denote the largest eigenvalue and the corresponding eigenvector of matrix* $\mathbf{B}^{-1}\mathbf{A}$*, respectively.*

By converting the average SINR expression into the form of Rayleigh quotient in Proposition 1, we can obtain the optimal beamforming vector in terms of the maximum SINR criterion, namely,

$$\mathbf{w}_{k,opt} = \mathbf{v}_{\max}\left(\mathbf{B}_{\mathrm{k}}^{-1}\mathbf{A}_k\right), \quad (19)$$

where $\mathbf{A}_k = \mathbf{C}\mathbf{R}_k\mathbf{C}^H$ and $\mathbf{B}_k = \mathbf{C}(\sum_{j=1,j\neq k}^{K} p_j \mathbf{R}_j)\mathbf{C}^H + \sigma^2 \mathbf{I}_N$. Here, $\lambda_{\max}(\cdot)$ and $\mathbf{v}_{\max}(\cdot)$ represent the maximum eigenvalue and corresponding eigenvector of the matrix.

By substituting (19) into (11), after some algebraic manipulations, we have

$$\gamma_k^{\max} = \frac{p_i \left|\mathbf{w}_{k,opt}^H \mathbf{h}_k\right|^2}{\sum_{j=1,j\neq k}^{K} p_j \left|\mathbf{w}_{k,opt}^H \mathbf{h}_j\right|^2 + \sigma^2} = \frac{\gamma_k^S}{\gamma_k^I + 1}, \quad (20)$$

where $\gamma_k^S = p_k|\mathbf{w}_{k,opt}^H \mathbf{h}_k|^2/\sigma^2$, $\gamma_k^I = \sum_{j=1,j\neq k}^{K}(p_j \gamma_{k,j}^I/\sigma^2) = \sum_{j=1,j\neq k}^{K} \overline{\gamma}_{k,j}^I |\widetilde{\mathbf{h}}_j|^2$, with $\overline{\gamma}_k^S = p_k|\mathbf{w}_{k,opt}^H \mathbf{C}\mathbf{R}_k^{1/2}|^2/\sigma^2$, $\overline{\gamma}_{k,j}^I = p_j|\mathbf{w}_{k,opt}^H \mathbf{C}\mathbf{R}_j^{1/2}|^2/\sigma^2$ representing the average SNR of each link.

3. Channel Statistical Property

This section studies the statistical properties of each link, which will be used in the subsequent derivations. First, the probability density function (PDF) of γ_k^S is given by [23]

$$f_{\gamma_k^S}(x) = \frac{1}{\overline{\gamma}_k^S} \exp\left(-\frac{x}{\overline{\gamma}_k^S}\right). \quad (21)$$

To obtain the PDF of $\gamma_k^I = \sum_{j=1,j\neq k}^{K} \overline{\gamma}_{k,j}^I |\widetilde{\mathbf{h}}_j|^2 = \sum_{j=1,j\neq k}^{K} \gamma_{k,j}^I$, we first have

$$f_{\gamma_{k,j}^I}(x) = \frac{1}{\overline{\gamma}_{k,j}^I} \exp\left(-\frac{x}{\overline{\gamma}_{k,j}^I}\right). \quad (22)$$

Then, following methods similar to those in [24], $f_{\gamma_k^I}(x)$ can be derived as

$$f_{\gamma_k^I}(x) = \sum_{p=1}^{t}\sum_{q=1}^{v_p} \frac{C_{p,q}}{\Gamma(q)\left(\overline{\gamma}_{k,q}^I\right)^q} x^{q-1} \exp\left(-\frac{x}{\overline{\gamma}_{k,p}^I}\right). \quad (23)$$

Based on (20), the PDF of $\gamma_k^{\max}$ is given by

$$f_{\gamma_k^{\max}}(x) = \int_0^\infty (y+1)\, f_{\gamma_k^S}(x(y+1))\, f_{\gamma_k^I}(y)\, dy. \quad (24)$$

Hence, by substituting (21) and (23) into (24), we have

$$\begin{aligned} &f_{\gamma_k^{\max}}(x) \\ &= \frac{1}{\overline{\gamma}_k^S} \exp\left(-\frac{x}{\overline{\gamma}_k^S}\right) \sum_{p=1}^{t}\sum_{q=1}^{v_p} \frac{C_{p,q}}{\Gamma(q)\left(\overline{\gamma}_{k,p}^I\right)^q} \\ &\quad \times \int_0^\infty \left(y^q + y^{q-1}\right) \exp\left(-\frac{xy}{\overline{\gamma}_k^S} - \frac{y}{\overline{\gamma}_{k,p}^I}\right) dy. \end{aligned} \quad (25)$$

By using [25, eq. (3.351.3)] along with the identity [26, eq. (10)], the PDF of $\gamma_k^{\max}$ can be expressed as

$$\begin{aligned} f_{\gamma_k^{\max}}(x) &= \frac{1}{\overline{\gamma}_k^S} \exp\left(-\frac{x}{\overline{\gamma}_k^S}\right) \sum_{p=1}^{t}\sum_{q=1}^{v_p} \frac{C_{p,q}}{\Gamma(q)} \\ &\quad \times \left(\overline{\gamma}_{k,p}^I \mathrm{G}_{1,1}^{1,1}\left[\frac{\overline{\gamma}_{k,p}^I x}{\overline{\gamma}_k^S}\middle| \begin{matrix} -q \\ 0 \end{matrix}\right] \right. \\ &\quad \left. + \mathrm{G}_{1,1}^{1,1}\left[\frac{\overline{\gamma}_{k,p}^I x}{\overline{\gamma}_k^S}\middle| \begin{matrix} -q+1 \\ 0 \end{matrix}\right]\right), \end{aligned} \quad (26)$$

where $\mathrm{G}_{p,q}^{m,n}\left[\cdot\middle|\cdot\right]$ denotes the Meijer-G function of a single variable [26].

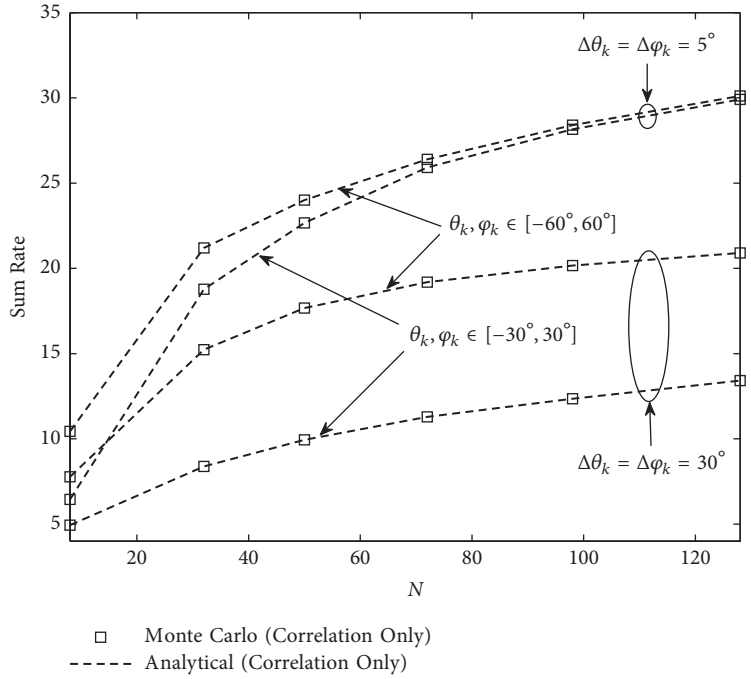

Figure 2: Achievable sum rate versus N for different combinations of AOA coverage areas and angular spreads.

4. Achievable Sum Rate

The ergodic achievable rate of the k-th user is given by [24, 27]

$$\begin{aligned} C_k &= E\left[\log_2\left(1+\gamma_k^{\max}\right)\right] \\ &= \frac{1}{\ln 2}\int_0^\infty \ln(1+x)\, f_{\gamma_k^{\max}}(x)\, dx. \end{aligned} \tag{27}$$

Utilizing (26) in (27) and applying the Meijer-G function representation of $\ln(1+x)$ [26, eq. (11)],

$$\ln(1+x) = \mathrm{G}_{2,2}^{1,2}\left[\, x \,\middle|\, \begin{matrix} 1,1 \\ 1,0 \end{matrix} \right], \tag{28}$$

we obtain the closed-form expression of R_k as

$$\begin{aligned} C_k = \exp\left(-\frac{x}{\overline{\gamma}_k^S}\right) \sum_{p=1}^{t}\sum_{q=1}^{\nu_p} \frac{C_{p,q}}{\Gamma(q)} \\ \times \left(\overline{\gamma}_k^S \mathrm{G}_{1,[1:2],0,[1:2]}^{1,1,2,1,1} \left[\begin{matrix} \overline{\gamma}_{k,p}^I \\ \overline{\gamma}_k^S \end{matrix} \middle| \begin{matrix} 1 \\ -q;1,1 \\ -- \\ 0;1,0 \end{matrix} \right] \right. \\ \left. + \overline{\gamma}_k^S \mathrm{G}_{1,[1:2],0,[1:2]}^{1,1,2,1,1} \left[\begin{matrix} \overline{\gamma}_{k,p}^I \\ \overline{\gamma}_k^S \end{matrix} \middle| \begin{matrix} 1 \\ -q+1;1,1 \\ -- \\ 0;1,0 \end{matrix} \right] \right), \end{aligned} \tag{29}$$

where $\mathrm{G}_{1,[1:2],0,[1:2]}^{1,1,2,1,1}\left[\,\cdot\,\middle|\,\cdot\,\right]$ represents the Meijer-G functions of two variables [28]. In deriving (29), we have applied [29, eq. 2.6.2)]. Hence, the total achievable sum rate for all the K users can be obtained by

$$C = \sum_{k=1}^{K} C_k, \tag{30}$$

where the exact results can be accordingly obtained from (29) with algebraic manipulations.

5. Numerical Results

In this section, we investigate the validity of the performance analysis and the effect of mutual coupling and antenna correlation on the LS-MIMO system through numerical simulations. Here, without loss of generality, the simulation parameters are chosen as follows: the ratio between the length and width of the URA is $a/b = 2$, element distance $d_x = d_y = d$, and $l = \lambda/2$, $Z_A = Z_T = 50\Omega$ [13], and the transmit SNR is 10dB. In addition, the K users are uniformly distributed in both the azimuth and elevation directions, and the number of multipath components per user is $L_k = 10$, the number of users is $K = 5$, and the Monte Carlo simulations are obtained by averaging over 10^6 channel realizations.

Figure 2 illustrates the achievable sum rate of the uplink multiuser large-scale MIMO system versus the number of antennas N for different AOAs and angular spreads. Here, the AOAs are assumed to satisfy $\theta_k, \varphi_k \in [-30^\circ, 30^\circ]$ or $\theta_k, \varphi_k \in [-60^\circ, 60^\circ]$, and the angular spreads are set as $\Delta\theta_k = \Delta\varphi_k = 5^\circ$ or $\Delta\theta_k = \Delta\varphi_k = 30^\circ$, which denote the low and high antenna correlation, respectively. As can be observed, the theoretical results obtained in (30) agree well with the Monte Carlo simulations, which validates our derived sum rate expressions. Meanwhile, it can also be found that the

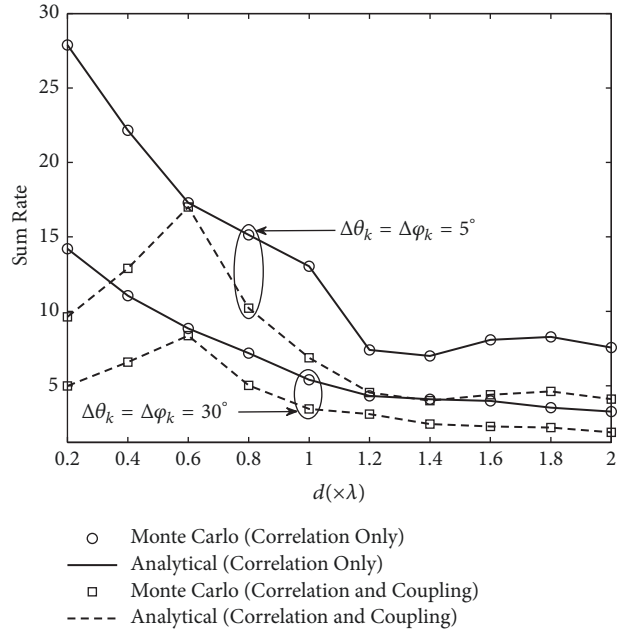

Figure 3: Achievable sum rate versus interelement spacing for a fixed array size.

achievable sum rate decreases with the increase in angular spread, implying that the performance of LS-MIMO can be improved with more correlated channels, when statistical CSI is used to fulfill optimal precoding.

By considering a fixed array with size of $4\lambda \times 2\lambda$, Figure 3 plots the achievable sum rate versus interelement spacing for different angular spreads with $\theta_k, \varphi_k \in [-30^\circ, 30^\circ]$. The numbers of antennas in each row and column of the array are calculated as $N_x = \lfloor 4\lambda/d \rfloor + 1$ and $N_y = \lfloor 2\lambda/d \rfloor + 1$. The fluctuation of curves is due to the up-and-down of mutual impendence when antenna distance increases [30]. It is observed that when only the antenna correlation is taken into account (Correlation Only), an increase in the element spacing, which corresponds to a decrease in the number of antennas and the antenna correlation, leads to a decrease in the achievable sum rate. On the other hand, for the cases where both antenna correlation and mutual coupling are considered (Correlation and Coupling), the maximal achievable sum rate is obtained when $d = 0.6\lambda$. Although more antenna elements can be deployed with associated higher antenna correlation in the presence of smaller interelement spacing, the mutual coupling becomes dominant factor and reduces the sum rate of the system. In addition, the number of antennas and channel correlation are reduced with an increase in the interelement spacing with the array size fixed. With these two competing factors, $d = 0.6\lambda$ is the best choice in terms of the achievable sum rate.

6. Conclusions

In this paper, we have investigated the achievable sum rate of a multiuser large-scale MIMO system taking into account mutual coupling and antenna correlation. Specifically, with optimal SINR-based beamforming at the BS, an exact closed-form expression for the system sum rate is derived in terms of Meijer-G functions of one or two variables, which provides an efficient approach to indicate the impact of various key parameters on the system performance. Simulations validate the theoretical results and also show the favorable conditions for achievable sum rate when both antenna correlation and mutual coupling are considered.

Data Availability

The MATLAB code data used to support the findings of this study were supplied by NSFC 61471392 under license and so cannot be made freely available. Requests for access to these data should be made to Prof. Yusheng Li.

Conflicts of Interest

The authors declare that they have no conflicts of interest.

Acknowledgments

This work is supported by the Research Project of NUDT under grant ZK18-02-11 and the National Natural Science Foundation of China under Grant 61471392.

References

[1] D. Gesbert, M. Kountouris, R. W. Heath, C.-B. Chae, and T. Sälzer, "Shifting the MIMO paradigm," *IEEE Signal Processing Magazine*, vol. 24, no. 5, pp. 36–46, 2007.

[2] L. Lu, G. Y. Li, A. L. Swindlehurst, A. Ashikhmin, and R. Zhang, "An overview of massive MIMO: benefits and challenges," *IEEE Journal of Selected Topics in Signal Processing*, vol. 8, no. 5, pp. 742–758, 2014.

[3] H. Q. Ngo, E. G. Larsson, and T. L. Marzetta, "The multicell multiuser MIMO uplink with very large antenna arrays and a finite-dimensional channel," *IEEE Transactions on Communications*, vol. 61, no. 6, pp. 2350–2361, 2013.

[4] T. L. Marzetta, "Noncooperative cellular wireless with unlimited numbers of base station antennas," *IEEE Transactions on Wireless Communications*, vol. 9, no. 11, pp. 3590–3600, 2010.

[5] H. Q. Ngo, E. G. Larsson, and T. L. Marzetta, "Energy and spectral efficiency of very large multiuser MIMO systems," *IEEE Transactions on Communications*, vol. 61, no. 4, pp. 1436–1449, 2013.

[6] M. Lin, L. Yang, W. Zhu, and M. Li, "An open-loop adaptive space-time transmit scheme for correlated fading channels," *IEEE Journal of Selected Topics in Signal Processing*, vol. 2, no. 2, pp. 147–158, 2008.

[7] S. Durrani and M. E. Bialkowski, "Effect of mutual coupling on the interference rejection capabilities of linear and circular arrays in CDMA systems," *IEEE Transactions on Antennas and Propagation*, vol. 52, no. 4, pp. 1130–1134, 2004.

[8] A. M. Tulino, A. Lozano, and S. Verdu, "Impact of antenna correlation on the capacity of multiantenna channels," *IEEE Transactions on Information Theory*, vol. 51, no. 7, pp. 2491–2509, 2005.

[9] M. Ivrlac, W. Utschick, and J. Nossek, "Fading correlations in wireless MIMO communication systems," *IEEE Journal on*

Selected Areas in Communications, vol. 21, no. 5, pp. 819–828, 2003.

[10] Z. Xu, S. Sfar, and R. S. Blum, "Receive antenna selection for closely-spaced antennas with mutual coupling," *IEEE Transactions on Wireless Communications*, vol. 9, no. 2, pp. 652–661, 2010.

[11] B. Clerckx, C. Craeye, D. Vanhoenacker-Janvier, and C. Oestges, "Impact of antenna coupling on 2 × 2 MIMO communications," *IEEE Transactions on Vehicular Technology*, vol. 56, no. 3, pp. 1009–1018, 2007.

[12] P. S. Taluja and B. L. Hughes, "Diversity limits of compact broadband multi-antenna systems," *IEEE Journal on Selected Areas in Communications*, vol. 31, no. 2, pp. 326–337, 2013.

[13] Y. Liu, B. Ai, and B. Chen, "Impact of mutual coupling on LTE-R MIMO capacity for antenna array configurations in high speed railway scenario," in *Proceedings of the 83rd IEEE Vehicular Technology Conference, VTC Spring 2016*, pp. 1–5, China, May 2016.

[14] X. Chen, S. Zhang, and Q. Li, "A review of mutual coupling in MIMO systems," *IEEE Access*, vol. 6, pp. 24706–24719, 2018.

[15] C. Masouros, M. Sellathurai, and T. Ratnarajah, "Large-scale MIMO transmitters in fixed physical spaces: the effect of transmit correlation and mutual coupling," *IEEE Transactions on Communications*, vol. 61, no. 7, pp. 2794–2804, 2013.

[16] H. Wei, D. Wang, H. Zhu, J. Wang, S. Sun, and X. You, "Mutual coupling calibration for multiuser massive MIMO systems," *IEEE Transactions on Wireless Communications*, vol. 15, no. 1, pp. 606–619, 2016.

[17] X. Xie, Y. Xu, H. Zhu, Q. Ling, X. Wang, and X. Luo, "Frugal calibration of mutual coupling in large scale antenna array," in *Proceedings of the 13th IEEE International Wireless Communications and Mobile Computing Conference, IWCMC 2017*, pp. 593–598, Spain, June 2017.

[18] P. Ioannides and C. A. Balanis, "Uniform circular and rectangular arrays for adaptive beamforming applications," *IEEE Antennas and Wireless Propagation Letters*, vol. 4, no. 1, pp. 351–354, 2005.

[19] R. Zi, X. Ge, H. Wang, J. Zhang, and C. Wang, "Multiuser massive MIMO uplink performance with mutual coupling effects," in *Proceedings of the IEEE Global Communications Conference*, pp. 3296–3301, Austin, Tex, USA, December 2014.

[20] F. B. Gross, *Smart Antennas for Wireless Communications*, McGraw-Hill Companies Inc, 2005.

[21] M. Lin and L. Yang, "Blind calibration and DOA estimation with uniform circular arrays in the presence of mutual coupling," *IEEE Antennas and Wireless Propagation Letters*, vol. 5, no. 1, pp. 315–318, 2006.

[22] G. H. Golub and C. F. Van Loan, *Matrix Computations*, The Johns Hopkins University Press, Baltimore, Md, USA, 3rd edition, 1996.

[23] K. An, M. Lin, J. Ouyang, and W.-P. Zhu, "Secure transmission in cognitive satellite terrestrial networks," *IEEE Journal on Selected Areas in Communications*, vol. 34, no. 11, pp. 3025–3037, 2016.

[24] K. An, T. Liang, G. Zheng, X. Yan, Y. Li, and S. Chatzinotas, "Performance limits of cognitive uplink FSS and terrestrial FS for Ka-band," *IEEE Transactions on Aerospace and Electronic Systems*, 2018.

[25] I. S. Gradshteyn and I. M. Ryzhik, *Table of Integrals, Series, and Products*, Academic Press, 2007.

[26] V. S. Adamchik and O. I. Marichev, "The algorithm for calculating integrals of hypergeometric type functions and its realization in REDUCE system," in *Proceedings of the International Symposium on Symbolic and Algebraic Computation*, pp. 212–224, Tokyo, Japan, August 1990.

[27] W. Lu, K. An, and T. Liang, "Robust beamforming design for sum secrecy rate maximization in multibeam satellite systems," *IEEE Transactions on Aerospace and Electronic Systems*, vol. 55, no. 3, 2019.

[28] I. S. Ansari, S. Al-Ahmadi, F. Yilmaz, M.-S. Alouini, and H. Yanikomeroglu, "A new formula for the BER of binary modulations with dual-branch selection over generalized-K," *IEEE Transactions on Communications*, vol. 59, no. 10, pp. 2654–2658, 2011.

[29] R. P. Agarwal, "Certain transformation formulae and Meijer's G function of two variables," *Indian Journal of Pure and Applied Mathematics*, vol. 1, no. 4, pp. 537–551, 1970.

[30] C. A. Balanis, *Antenna Theory: Analysis and Design*, John Wiley and Sons, 2012.